Available online at www.sciencedirect.com
ScienceDirect
Surface & Coatings Technology 201 (2007) 8348–8351
SURFACE & COATINGS TECHNOLOGY
www.elsevier.com/locate/surfcoat

Fabrication of highly (1000) oriented textured zinc oxide films by metal cathodic arc and oxygen dual plasma deposition and their optical properties

Y.F. Mei [a], Ricky K.Y. Fu [a], G.G. Siu [a], Paul K. Chu [a,*], Z.M. Li [b], C.L. Yang [b], W.K. Ge [b], Z.K. Tang [b], W.Y. Cheung [c], S.P. Wong [c]

[a] Department of Physics and Materials Science, City University of Hong Kong, Kowloon, Hong Kong, China
[b] Department of Physics, Hong Kong University of Science & Technology, Clear Water Bay, Kowloon, Hong Kong, China
[c] Department of Electronic Engineering, Chinese University of Hong Kong, Shatin, Hong Kong, China

Available online 13 March 2007

Abstract

Highly (1000) oriented ZnO films were successfully grown onto silicon substrates using a dual plasma deposition process incorporating a metal cathodic arc source and oxygen ambient. The optical properties of a series of ZnO films deposited on quartz using similar conditions were investigated using UV–visible spectrophotometry, and the effects on the band gap were investigated. The absorption of C-excitons resulting in a blue-shift of the band gap at room temperature is accentuated due to strong absorption at higher energy for light polarized ($\boldsymbol{E}//c$) in the highly (1000) oriented ZnO film.

PACS: 71.55.Gs; 68.55.Jk; 78.20.Ci
Keywords: Zinc oxide; Cathodic arc; Plasma deposition; Optical properties

1. Introduction

Zinc oxide (ZnO) films possess many interesting characteristics such as piezoelectric effects [1], conductive effects [2], acoustic characteristics [3], direct band gap (3.3 eV), and absence of toxicity. The materials have thus attracted much attention because of their potential use in optoelectronic devices such as solar cells and displays [4]. Different methods have been proposed to synthesize ZnO films including chemical vapor deposition (CVD) [5], thermal oxidation [6], radio frequency (RF) magnetron sputtering [7], pulsed laser deposition [8], electron beam evaporation [9], spray pyrolysis [10], and electrodeposition [11]. Recently, fabrication of ZnO films by the filtered cathodic vacuum arc (FCVA) technique has aroused interest because of the readily adjustable deposition parameters, low growth temperature, and convenient in-situ doping using an overlying plasma [12]. Furthermore, the high kinetic energies of the precursors produced by the FCVA technique are believed to play a key role in the realization of low temperature deposition.

We have recently attempted to deposit ZnO films using hybrid plasma deposition in an immersion configuration. In this method, a zinc cathode is triggered to produce the zinc plasma, and oxygen gas is simultaneously fed into the chamber [13]. The zinc plasma is guided through a curved magnetic duct to eliminate deleterious macro-particles [14] and then transported into the processing chamber. The zinc plasma interacts with oxygen in the vacuum chamber and a dual zinc–oxygen plasma is formed to conduct deposition. Using this technique, highly (1000) oriented ZnO films were fabricated on silicon substrates. The optical properties of another series of ZnO films deposited on fused quartz employing similar conditions were investigated using UV–visible spectrophotometry. The absorption of the C-exciton resulting in a blue-shift of the band gap at room

* Corresponding author. Tel.: +852 27887724; fax: +852 27889549.
E-mail address: paul.chu@cityu.edu.hk (P.K. Chu).

0257-8972/$ - see front matter © 2007 Elsevier B.V. All rights reserved.
doi:10.1016/j.surfcoat.2006.10.056

temperature was observed to be accentuated due to the (1000) orientation ($a//n$) of the ZnO film and other effects are discussed in this paper.

2. Experimental details

The substrates used in our experiment were p-type (1000) silicon wafers with a resistivity of 10–30 Ω·cm and fused quartz glass. The base pressure in the vacuum chamber of our plasma immersion ion implanter equipped with a cathodic arc vacuum arc source was about 1×10^{-5} Torr [15–17]. The zinc plasma was formed by the cathodic arc source, guided through a magnetic filter to reduce detrimental macro-particles, and drifted into the vacuum chamber. Oxygen gas (flow rate: 20 sccm; pressure: $\sim1.0\times10^{-3}$ Torr) was simultaneously bled into the vacuum chamber during deposition and interacted with the drifting zinc plasma thereby producing a dual plasma consisting of both zinc and oxygen ions. The samples that were biased to −300 V were positioned about 10–20 cm from the exit of the plasma stream. Samples A and B consisting of ZnO deposited on Si substrates at a substrate bias of −300 V were positioned at different distances from the plasma source (10 cm for sample A and 20 cm for sample B). The experimental conditions used to prepare samples 1 and 4 were similar to those of samples A and B, except that the substrates were fused quartz. Sample 2 was produced using a bias of −100 V which shifted the crystal orientation of the film. With regard to sample 3, a small amount of N was incorporated into the ZnO film at a bias of −300 V. Rutherford backscattering spectrometry (RBS) was performed on the samples using a 2 MeV $^4He^{++}$ beam and a backscattering angle of 170° to determine the film thickness as well as the Zn and O contents. The growth rates were 1.0–2.1 nm/min.

3. Results and discussion

The typical XRD patterns acquired from two ZnO films deposited on Si at distances of 10 cm (A) and 20 cm (B) are shown in Fig. 1. The two diffraction peaks observed around 31.2° and 64.9° are those of (1000) and (2000) ZnO, where the c axis is parallel to the substrate surface. A weak peak around 28.1° can be attributed to (002) Si. The sharp and intense (1000) and (2000) peaks indicate that the films are highly oriented. Insets (a) and (b) present a typical surface AFM (atomic force microscopy) and cross-sectional SEM (scanning electron microscopy) images of the film B. The film has a very smooth surface with a root mean square (rms) roughness of about 3 nm. Based on the cross-sectional image shown in inset (b), it can be inferred that textured deposition onto Si has been conducted successfully.

Although the optical band gap in ZnO single crystals has been documented [18], there are substantial variations as a result of the distortion of the band gap due to factors such as the grain size [19], positive charge of the donor atoms [20], thermal mismatch and strain between the film and substrate [20,21], Burstein–Moss (BM) effect [22], and C-exciton absorption [23]. In order to investigate the band gap of our ZnO films, various types of ZnO films were fabricated on fused quartz using similar parameters and then characterized utilizing UV–visible spectrophotometry. The XRD patterns of these samples are shown in Fig. 2. The inset shows α^2 as a function of incident radiation and the band gap is determined by extrapolating the linear portion of the curve. The film parameters are shown in Table 1. The band edge of the (100) ZnO structure (No. 4, 3.405 eV) is larger by 61 meV than that of (0002) ZnO film on fused quartz (No. 1, 3.344 eV). Quantum confinement effects

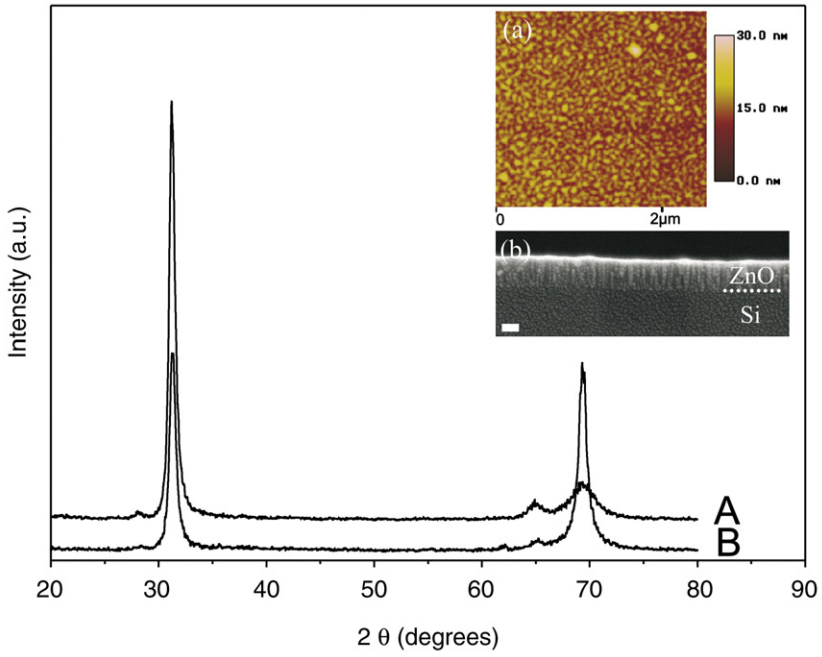

Fig. 1. X-ray diffraction patterns obtained from ZnO films deposited on Si at two different distances (A: 10 cm and B: 20 cm). Shown in inset (a) is the surface AFM micrograph and inset (b) the cross-sectional SEM micrograph [the scale bar is 100 nm] of sample B.

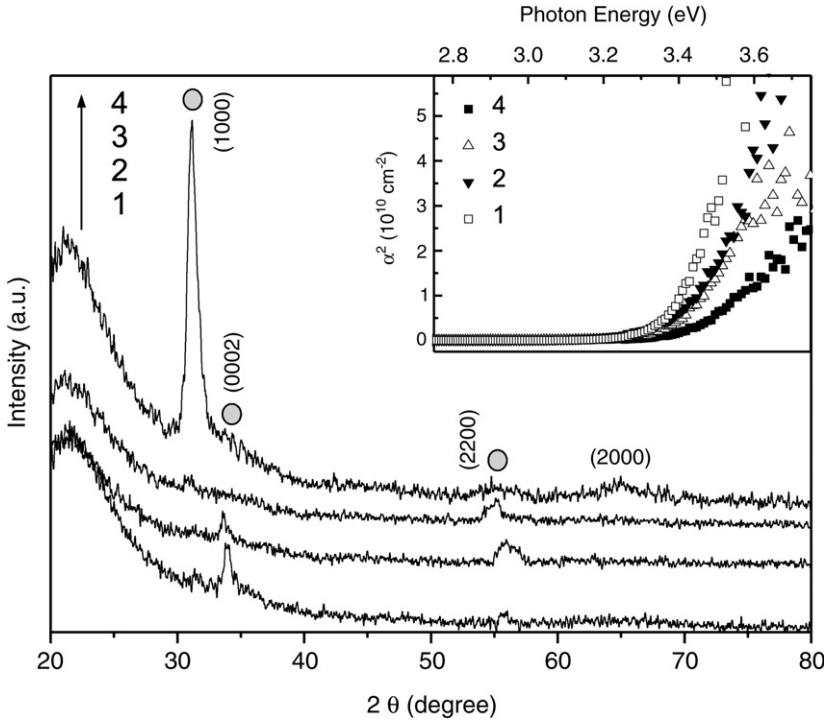

Fig. 2. XRD patterns acquired from ZnO films deposited on fused quartz. No. 4 and No. 1 were fabricated using a similar as samples A and B, respectively. No. 2 was produced using a DC sample bias −100 V and No. 3 was synthesized using a mixture of O_2 and N_2 at a DC bias of −300 V.

can be excluded here because of the large grain size (>100 nm) in our ZnO film (No. 4).

The modulation of the conduction and valence band edges due to the positive charge on the donor atoms should be considered first on account of the higher measured electron concentrations (No. 4: $1.02\times10^{20}/\mathrm{cm}^3$; No. 1: $3.14\times10^{19}/\mathrm{cm}^3$) and n-type conductivity. Consequently, the strength of this modulation, $2V_0$, follows from Poisson's equation: $2V_0=(2\pi e^2/\kappa_0)n_D(d_n/2)^2$ [24]. Here κ_0, e, n_D, and d_n stand for the static dielectric constant, elementary charge, donor concentration, and thickness of the film, respectively. The values of $2V_0$ are 19.76 meV and 2.68 meV for the (1000) (No. 4) and (2000) (No. 1) orientations, respectively. The shift between these two values is about −17.08 meV. It implies that the band gap is reduced due to the higher electron concentration in the (1000) ZnO film (No. 4) compared to that of (0002) (No. 1).

The thermal mismatch strain in the thin film may account for the blue shift of the band gap [20,21]. Adopting the treatment of the effects of stress on optical absorption, we can describe the position of the highest valence $[E_v(\Gamma_7^u)]$ in terms of the deformation potential as $\Delta E_v(\Gamma_7^u)=\delta_1+1.05\delta_2$, where, $\delta_1=C_1\varepsilon_{zz}+C_2(\varepsilon_{xx}+\varepsilon_{yy})$; $\delta_2=C_3\varepsilon_{zz}+C_4(\varepsilon_{xx}+\varepsilon_{yy})$, ε_{xx}, ε_{yy}, ε_{zz} are the strains in the principal crystallographic directions, and $C_1=-2.66$ eV, $C_2=2.82$ eV, $C_3=-1.34$ eV, and $C_4=1.0$ eV are the deformation potentials of ZnO. The in-plane strain is given by $\varepsilon_{ij}^{\mathrm{film}}=\int(\alpha_{ij}^{\mathrm{film}}-\alpha_{ij}^{\mathrm{substrate}})\mathrm{d}T$, where α_{ij} is the thermal expansion coefficient [ZnO: 6.5×10^{-6}/K (//a) and 3.7×10^{-6}/K (//c); fused quartz glass: 0.55×10^{-6}/K], $\varepsilon_{\text{out of plane}}=-\varepsilon_{\text{in-plane}}(c_{1133}+c_{2233})/c_{3333}$, and $c_{1133}=105.1$ GPa and $c_{3333}=210.9$ GPa represent the elastic stiffness of ZnO. In our experiments, the deposition temperature was about 200 °C. Hence, $\Delta E_v(\Gamma_7^u)$ can be determined to be about 9.6 and 14.2 meV for the (1000) and (0002) ZnO films on fused quartz, respectively. It should be noted that the difference between them (4.6 meV) is too small to explain the large blue shift (61 meV) observed in our experiments.

The conduction band edge is populated by excessive carriers donated by the impurities. It consequently leads to a blue shift of the optical band-to-band transitions, and it is known as the BM effect [25]. The BM shift is proportional to $n_D^{2/3}$ and it is inversely proportional to the effective mass of the band when a parabolic band is assumed near the minimum of the conduction band [22]. However, this effect is not pronounced in all our samples because of the abnormal conductivities of Nos. 2 and 3.

It is well known that there are intrinsic excitons $A_{\mathbf{n}}$, $B_{\mathbf{n}}$, and $C_{\mathbf{n}}$ at low temperature, where **n** indicates the different quantum states [23]. The p-like valence band is split by the spin–orbit and crystal–field interactions. The valence–conduction band separations can be calculated as the exciton series limit assuming the $1/\mathbf{n}^2$ energy relation. It gives valence–band separations $E_{AB}=3.2$ meV and $E_{BC}=39.3$ meV. For light polarized $\boldsymbol{E}//c$, strong absorption peaks have been observed at energies greater than the band gap in ZnO crystal even at room

Table 1
Parameters (crystal structures, electron concentration, and measured band gap) of the four ZnO films (Nos. 1, 2, 3, and 4) deposited on fused quartz

Sample orientation	No. 1	No. 2	No. 3	No. 4
(0002)	√	√		
(2200)	√ (weak)	√	√	
(1000)	√ (little)		√ (weak)	√ (strong)
n_d ($\times10^{20}/\mathrm{cm}^3$)	0.314	1.134	High resistance n-type	1.019
Band gap (eV)	3.344	3.379	3.369	3.405

temperature ($\mathbf{n}=1$) due to the C-exciton absorption [23]. When the incident light is unpolarized, strong absorption occurs because $\boldsymbol{E}$ is parallel to the c axis for the (1000) ZnO film. For light polarized $\boldsymbol{E}\perp c$, the absorption of C-exciton is weak, and so a large blue shift can be induced in the (1000) ZnO film compared to (0002). This effect can also be confirmed by the band gap of No. 2 and 3 because in the (2200) orientation, the c axis is at an angle to the surface.

The C-exciton absorption can be quite dominant and induce a blue shift, but the maximal effect should be about 39.3 meV. Therefore, the variation in the band gap may also be affected by the strain induced by the thermal mismatch [a small blue shift for (1000) ZnO film], BM effect (blue shift), and the effects of the positive charges on the donor atoms (red shift), depending on the properties of the ZnO films.

4. Conclusion

Highly (1000) oriented ZnO films have been successfully grown on silicon substrate utilizing a dual plasma deposition process. The optical properties of another series of ZnO films deposited on quartz using similar experimental conditions were investigated using UV–visible absorption spectroscopy. The absorption of C-exciton leads to a blue shift of band gap at room temperature and is a direct result of the (1000) orientation of the ZnO film.

Acknowledgements

The authors thank Mr. M. K. Tang and Dr. Amy X. Y. Lu for experimental assistance. This work was supported by the City University of Hong Kong Strategic Research Grant No. 7002138.

References

[1] B. Wacogne, M.P. Roe, T.A. Pattinson, C.N. Pannell, Appl. Phys. Lett. 67 (1995) 1674.
[2] B. Ismail, M.A. Abaab, B. Rezig, Thin Solid Films 383 (2001) 92.
[3] T. Mitsuya, S. Ono, K. Wase, J. Appl. Phys. 51 (1980) 2464.
[4] T. Ikeda, J. Sato, Y. Hayashi, Sol. Energy Mater. Sol. Cells 34 (1994) 379.
[5] J.S. Kim, H.A. Marzouk, P.J. Reocroft, C.E. Hamrin, Thin Solid Films 217 (1992) 133.
[6] P. Bonasewicz, W. Hirschwald, G. Neumann, Thin Solid Films 142 (1986) 77.
[7] Sang-Hun Jeong, B.-S. Kim, B.-T. Lee, Appl. Phys. Lett. 82 (2003) 2625.
[8] X.L. Wu, G.G. Siu, C.L. Fu, H.C. Ong, Appl. Phys. Lett. 78 (2001) 2285.
[9] A. Kuroyanagi, Jpn. J. Appl. Phys. 28 (1989) 219.
[10] M.G. Ambia, M.N. Islam, M.O. Hakim, J. Mater. Sci. 29 (1994) 6575.
[11] M. Izaki, T. Omi, Appl. Phys. Lett. 68 (1996) 2439.
[12] Y.G. Wang, S.P. Lau, H.W. Lee, S.F. Yu, B.K. Tay, X.H. Zhang, K.Y. Tse, H.H. Hng, J. Appl. Phys. 94 (2003) 1597.
[13] X.B. Tian, R.K.Y. Fu, P.K. Chu, J. Vac. Sci. Technol., A 20 (2002) 160.
[14] D.T.K. Kwok, T. Zhang, P.K. Chu, M.M.M. Bilek, A. Vizir, I.G. Brown, Appl. Phys. Lett. 78 (2001) 422.
[15] P.K. Chu, S. Qin, C. Chan, N.W. Cheung, L.A. Larson, Mater. Sci. Eng., R Rep. 17 (6–7) (1996) 207.
[16] P.K. Chu, B.Y. Tang, Y.C. Cheng, P.K. Ko, Rev. Sci. Instrum. 68 (1997) 1866.
[17] P.K. Chu, B.Y. Tang, L.P. Wang, X.F. Wang, S.Y. Wang, N. Huang, Rev. Sci. Instrum. 72 (2001) 1660.
[18] V. Srikant, D.R. Clarke, J. Appl. Phys. 83 (1998) 5447.
[19] T. Matsumoto, H. Kato, K. Miyamoto, M. Sano, E.A. Zhukov, T. Yao, Appl. Phys. Lett. 81 (2002) 1231.
[20] V. Srikant, D.R. Clarke, J. Appl. Phys. 81 (1997) 6357.
[21] G.E. Pikus, Sov. Phys., Solid State 6 (1964) 261.
[22] K.J. Kim, Y.R. Park, Appl. Phys. Lett. 78 (2001) 475.
[23] W.Y. Liang, A.D. Yoffe, Phys. Rev. Lett. 20 (1968) 59.
[24] G.H. Dohler, IEEE J. Quantum Electron. QE-22 (1986) 1682.
[25] E. Burstein, Phys. Rev. 93 (1954) 632;
T.S. Moss, Proc. Phys. Soc., London, Ser. B 67 (1954) 775.